CALIBRATION STANDARDS AND UNCERTAINTIES IN RADAR CROSS SECTION MEASUREMENTS*

Lorant A. Muth
National Institute of Standards and Technology
Boulder, CO 80303

Abstract — Standards for radar cross section measurements are being developed cooperatively by NIST and DoD scientists. Three technical areas were defined as the foundation of such an effort: (1) monostatic single-channel calibration, (2) full polarimetric calibration using a scattering matrix formalism, and (3) analysis of radar cross section calibration and measurement uncertainty. In this paper I review the results of assessment of calibration data accuracy using a set of cylinders as artifact standards, examine the theory of polarimetric calibrations, and discuss essential areas of radar cross section uncertainty analysis.

Key words: calibration, calibration artifacts, cylinders, dihedrals, model consistency, monostatic measurements, polarimetric measurements, radar cross section, uncertainty.

INTRODUCTION

The need for standards in radar cross section (RCS) measurements has been noted in 1965 [1]. The absence of uniform calibration and measurement procedures makes it difficult to compare RCS data objectively. The absence of a well-defined uncertainty procedure makes evaluation of the quality of RCS data difficult or impossible.

During the last five years, scientists at the National Institute of Standards and Technology (NIST) and DoD's Radar Cross Section Measurement Working Group (RCSMWG) have been collaborating to improve RCS measurements. A dual calibration technique using cylinders [2] has been proposed to provide a measure of calibration uniformity throughout the RCS community. At the same time, this technique also gives a measure of the magnitude of error in a monostatic single-channel calibration. Similarly, a modified analysis of the full polarimetric scattering matrix formalism, as applied to dihedrals, has been proposed [3 – 5] to improve the determination of channel cross-polarization ratios and to provide uncertainty estimates. Considerable research has been undertaken to provide a foundation and a general framework for RCS uncertainty analysis [7,8], but this work is still ongoing. I continue the discussion of RCS uncertainty analyses reported previously. In particular, I derive theoretical expressions for the upper-bound of uncertainty in the discrepancy obtained in the dual cylinder calibration technique.

CALIBRATION OF MONOSTATIC RADARS

Measurements on a set of precision cylinders mounted on their flat surfaces, shown in Figure 1, have been made at many RCS measurement ranges. The purpose is to assess RCS calibration accuracy within and across laboratories.

The RCS of a cylinder (for a fixed polarization and orientation) can be obtained by comparing the scattering relative to a known scatterer using the expression

$$\sigma_{i;j}(f) = \left| \frac{E_i^{(m)}(f)}{E_j^{(m)}(f)} \right|^2 \sigma_j^{(c)}(f), \qquad (1)$$

where the measured electric fields $E^{(m)}$ may have been derived by incorporating background subtraction techniques [2]. Here $\sigma_j^{(c)}$ is the *computed* cross section of cylinder j, and $\sigma_{i;j}$ is the measured cross section of cylinder i, when cylinder j is used to calibrate the measurement system.

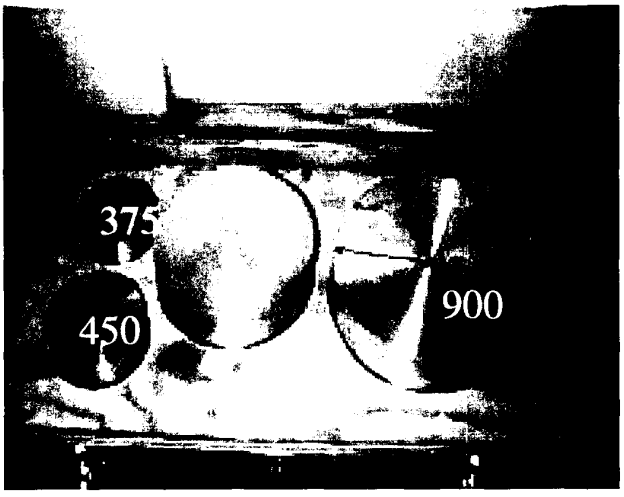

Figure 1. Standard cylinder set (shown with identification numbers) for monostatic RCS calibrations. For details, see [2] and [9]. (Courtesy of B. Kent, AFRL, WPAFB).

*A U.S. Government contribution, not subject to copyright in the United States.

0-7803-4977-6/99/$10.00 ©1999 IEEE

Two related measures of error are suggested [9]. First, we can state the *discrepancy* between measured and computed *(assumed exact)* σ, or, second, we can examine the interlaboratory variation using the normalized electric fields,

$$\Delta\sigma_{i;j} = 10\log(\sigma_{i,j}/\sigma_i^{(c)}), \qquad (2a)$$

and

$$\mathcal{E}_{i;j}^{(l)} = 20\log(|E_i^{(l)}/E_j^{(l)}|), \qquad (2b)$$

where a laboratory is identified by the superscript l. The second measure eliminates the need to know the cross sections or to deal with errors in the computed cross sections.

Figure 2 shows results of comparisons between cylinders as a function of frequency from 2 to 18 GHz obtained using Equations (1) and (2a) for the vv polarization. Overall, the results are very encouraging with discrepancies no greater than ± 0.4 dB for $f > 3.5$ GHz. As expected the discrepancy at lower frequencies are greater than at higher frequencies, but not outside acceptable bounds. Similar results were obtained for the hh polarization. We must recognize here that discrepancy is not uncertainty; the uncertainty at each point in Figure 2 needs to be determined by independent procedures.

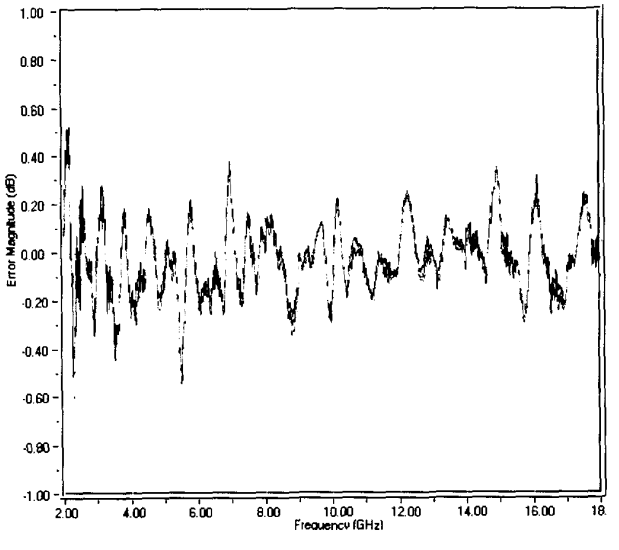

Figure 2. A monostatic RCS repeatability study for vv polarization. The *discrepancies* between the measured and computed RCS of three 450-cylinder targets (see Figure 1). A single 900-cylinder was used as the calibration artifact. (Courtesy of B. Kent, AFRL, WPAFB).

POLARIMETRIC CALIBRATION OF MONOSTATIC RADARS

The RCSMWG reported large unacceptable cross-polarimetric channel isolations when they implemented one of several similar but distinct techniques reported in the literature [4,5]. Most calibration procedures recommend (1) a dihedral as the primary calibration target, and (2) a two-point calibration technique. Other known calibration techniques are essentially variants of the basic procedure using dihedrals. In this section, I propose a continually rotating dihedral as a calibration device, as shown in Figure 3. As will be seen below, this calibration technique offers many improvements in calibration data diagnostics and analysis, and makes uncertainty analysis tractable.

When we calibrate a polarimetric radar system, we determine its transmitting and receiving characteristics using targets with known scattering matrices. In general, the *measured signal* $\hat{\mathcal{M}}$ scattered from a target is given by

$$\begin{pmatrix} 1 & \gamma_{hv} \\ \gamma_{vh} & \gamma_{vv} \end{pmatrix} \odot \begin{pmatrix} \hat{\mathcal{M}}_{hh} & \hat{\mathcal{M}}_{hv} \\ \hat{\mathcal{M}}_{vh} & \hat{\mathcal{M}}_{vv} \end{pmatrix} =$$

$$g_{hh}\mathcal{K} \begin{pmatrix} R_{hh} & R_{hv} \\ R_{vh} & R_{vv} \end{pmatrix} \begin{pmatrix} \mathcal{A}_{hh} & \mathcal{A}_{hv} \\ \mathcal{A}_{vh} & \mathcal{A}_{vv} \end{pmatrix} \begin{pmatrix} T_{hh} & T_{hv} \\ T_{vh} & T_{vv} \end{pmatrix}, \qquad (3)$$

where $\odot$ is the element-by-element Hadamard product [10], $\mathbf{R}$ and $\mathbf{T}$ are the receiving and transmitting characteristics of the radar system, $\mathcal{A}$ is the scattering matrix of the target, and $\mathcal{K}$ is a complex constant containing phase and distance information. The subscripts h and v refer to horizontal and vertical polarizations of the electric field vector of the signal; the right subscript indicates the polarization of an incoming signal, and the left subscript gives the polarization of the radar channel responding to the incoming signal. The relative amplifications $\gamma_{hv} = g_{hh}/g_{hv}$, $\gamma_{vh} = g_{hh}/g_{vh}$, and $\gamma_{vv} = g_{hh}/g_{vv}$, defined in terms of amplifications g_{pq}, p, $q = h$ or v that may be introduced before the received signal is recorded, can be determined as part of the calibration procedure. If $\mathcal{A}$ is known, we can perform measurements to determine $\mathbf{R}$ and $\mathbf{T}$ uniquely; that is, we can calibrate the radar system.

An important data integrity check follows from Equation (3). The determinant of the incoming signal matrix $\mathcal{M}$ satisfies the relationship $|\mathcal{M}| = \mathcal{K}^2|\mathbf{R}||\mathcal{A}||\mathbf{T}|$. If $|\mathcal{A}|$ is independent of target orientation, $|\mathcal{M}|$ is also independent of target orientation. However, if $g_{hh}g_{vv} - g_{hv}g_{vh} \neq 0$, then $|\hat{\mathcal{M}}|$ will not be constant under the same conditions, but the modified determinant $\epsilon\hat{\mathcal{M}}_{hh}\hat{\mathcal{M}}_{vv} - \hat{\mathcal{M}}_{hv}\hat{\mathcal{M}}_{vh}$ will be constant if we choose

$$\epsilon = \frac{g_{hv}g_{vh}}{g_{hh}g_{vv}}. \qquad (4)$$

A critical examination of published procedures leads to the understanding that new diagnostic and analysis tools are needed for better polarimetric RCS calibrations. We need to (1) *introduce special diagnostic techniques* to isolate and remove unwanted signals from the calibration data, (2) *verify the consistency* between the polarimetric calibration dataset and the system scattering model, (3)

of uncertainties have been assigned hypothetical values, and the less important entries have been assigned 0.0 dB for illustration only. Although the sources of uncertainties have been presented in various classification schemes [7,8], a complete theoretical treatment supported by a comprehesive set of measurements to determine uncertainties have not been developed yet. The complexity of the measurement system and the associated procedures make a full uncertainty analysis difficult and expensive.

Table 1.
RCS Calibration Target Uncertainties
For a Fixed Frequency and Orientation
(hypothetical estimates in decibels)

Average Illumination	0.7
Background – Target Interaction	0.0
Cross Polarization	0.0
Drift	0.3
Frequency	0.0
Integration	0.0
I-Q Imbalance	0.0
Near Field	0.0
Noise – Background	0.5
Nonlinearity	0.3
Range	0.0
Target Orientation	0.0
Reference RCS	0.0
Combined Uncertainty (RSS)	1.0

We can easily exhibit the presence of errors in Equation (1) explicitly. If $E_i^0,\ i = 1,2$ *is the scattered monostatic field due to a plane wave illumination*, then by definition

$$\left|\frac{E_2^0}{E_1^0}\right|^2 \frac{\sigma_1^0}{\sigma_2^0} = 1, \tag{11}$$

where σ_i^0, are the computed radar cross sections of the targets. *We assume for now that the computations yielded theoretically correct results.* The measured electric field is

$$\hat{E} = E^0 + \Delta E, \tag{12}$$

where ΔE is the total measured error field. We define the *fractional error fields* for the target and calibration artifacts as

$$\Delta_i \equiv \frac{\Delta E_i}{E_i^0}, \tag{12}$$

where $\Delta E_i,\ i = 1,2$ are the sum of the received scattered error fields. *These error fields are primarily due to the scattering of the bistatic illumination of the target and to the bistatic response of the target to the plane wave illumination.* In general, all other sources of uncertainty listed in Table 1 contribute to the error fields. Thus,

$$\Delta E = \Delta E_{bi} + \Delta E_{tmi} + \Delta E_o + \Delta E_n + \cdots, \tag{13}$$

where the subscripts denote the *error signals* due to bistatic, target-mount interaction, orientation and noise, respectively. It is assumed that system drift and nonlinearity has been appropriately corrected for. If $\Delta\sigma_i$ is the measurement error in σ_i^0, then the *discrepancy* e between the measured and computed (error-free) radar cross sections is given by the *discrepancy equation*

$$e \equiv 1 + \frac{\Delta\sigma_2}{\sigma_2^0} = \frac{\left|1 + \Delta_2\right|^2}{\left|1 + \Delta_1\right|^2}, \tag{14a}$$

For $|\Delta_1| < 1$ and $|\Delta_2| < 1$, the *first-order* approximation to Equation (14a) is

$$e \equiv 1 + \frac{\Delta\sigma_2}{\sigma_2^0} \approx \left|1 + \Delta_2 - \Delta_1\right|^2, \tag{14b}$$

which implies that all the uncertainties in the two measurements add [6]. This method of combination of uncertainties have been presented in [7], where the root-sum-square (RSS) was chosen to determine the overall measurement uncertainty [6]. Alternatively, we can choose to combine all uncertainties in a simple sum to obtain upper bound uncertainties [6].

The contours of measurement discrepancies defined in Equation (14) are plotted in Figure 4. From Equation (14a) we observe that a parameter useful for characterization of RCS measurement ranges for a particular combination of calibration and test targets is the the complex *fractional error field ratio*

$$\beta_{21} \equiv \frac{\Delta_2}{\Delta_1}. \tag{15}$$

Clearly, if $\beta_{21} = 1$, then $\Delta\sigma_2 = 0$, which demonstrates that *measurement discrepancies are a consequence of the difference in the fractional error field scattering characteristics of the calibration and unknown targets and their interactions with the environment. Such differences could be approximated by numerical modeling, and could be used in the prediction of error bounds for RCS measurements.* We observe that for repeated measurements made on the same calibration artifact, β_{21} provides a measure of the repeatability of a measurement sequence.

simplify the data-analysis technique, and (4) *specify the uncertainty* in the calibration procedure.

These objectives can be achieved by a polarimetric calibration procedure where we use a *rotating* dihedral as the primary target to obtain a complete polarimetric dataset as the dihedral rotates through a full 360°. Since the high-frequency scattering matrix $\mathcal{A}$ of a dihedral (neglecting diffraction) is given by

$$\mathcal{K}_d \begin{pmatrix} -\cos 2\theta & \sin 2\theta \\ \sin 2\theta & \cos 2\theta \end{pmatrix}, \tag{5}$$

where θ is the angle of rotation around the line of sight (z axis), special *diagnostic* explorations of the dataset to detect system problems, based on the symmetries of the dihedral, become straightforward. The calibration equation now becomes, assuming the reciprocity condition $\mathbf{R} = \tilde{\mathbf{T}}$,

$$\begin{pmatrix} 1 & \delta_{hv} \\ \delta_{vh} & \delta_{vv} \end{pmatrix} \odot \begin{pmatrix} \hat{\mathcal{M}}_{hh} & \hat{\mathcal{M}}_{hv} \\ \hat{\mathcal{M}}_{vh} & \hat{\mathcal{M}}_{vv} \end{pmatrix} = \tag{6}$$

$$g_{hh} R_{hh}^2 \mathcal{K}\mathcal{K}_d \begin{pmatrix} 1 & \epsilon_h \\ \epsilon_v & 1 \end{pmatrix} \begin{pmatrix} -\cos 2\theta & \sin 2\theta \\ \sin 2\theta & \cos 2\theta \end{pmatrix} \begin{pmatrix} 1 & \epsilon_v \\ \epsilon_h & 1 \end{pmatrix},$$

where $\rho = R_{vv}/R_{hh}$, $\delta_{hv} = \gamma_{hv}/\rho$, $\delta_{vh} = \gamma_{vh}/\rho$, and $\delta_{vv} = \gamma_{vv}/\rho^2$; $\epsilon_h = R_{hv}/R_{hh}$, and $\epsilon_v = R_{vh}/R_{vv}$. We also define $\delta_{hh} = g_{hh} R_{hh}^2$.

The matrix elements in Equation (6) have the general form, with $p,\ q = h$ or v,

$$\hat{\mathcal{M}}_{pq} = C_{pq} \cos 2\theta + S_{pq} \sin 2\theta, \tag{7}$$

These components are not independent, since we must satisfy the conditions that $|M|$ and the modified determinant $\epsilon \hat{\mathcal{M}}_{hh}\hat{\mathcal{M}}_{vv} - \hat{\mathcal{M}}_{hv}\hat{\mathcal{M}}_{vh}$ be independent of θ. This will be true only if the 8 Fourier coefficients in Equation (7) satisfy the nonlinear constraint

$$\frac{C_{hv}S_{vh} + S_{hv}C_{vh}}{C_{hh}S_{vv} + S_{hh}C_{vv}} = \frac{C_{hv}C_{vh} - S_{hv}S_{vh}}{C_{hh}C_{vv} - S_{hh}S_{vv}}. \tag{8}$$

We can show that each side of Equation (8) is really ϵ defined in Equation (4).

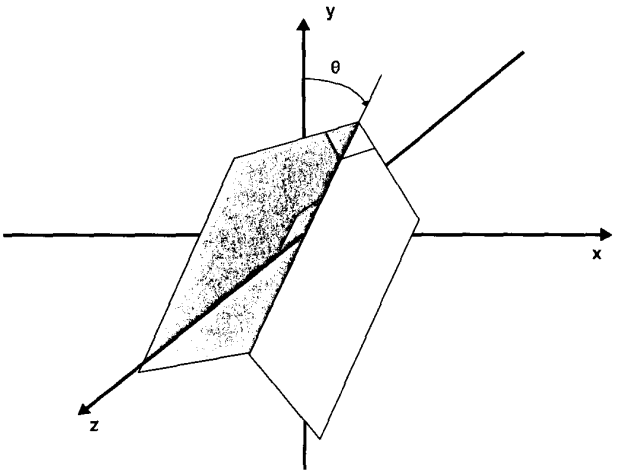

Figure 3. The standard dihedral used in monostatic polarimetric RCS calibrations. The z axis of the rotating coordinate system is along the line of sight to the radar.

Once the Fourier coefficients are obtained, we can solve for all polarimetric radar system parameters. Thus,

$$-\frac{2\epsilon_h}{1-\epsilon_h^2} = \frac{S_{hh}}{C_{hh}}, \qquad \text{and} \qquad \frac{2\epsilon_v}{1-\epsilon_v^2} = \frac{S_{vv}}{C_{vv}} \tag{9}$$

yield ϵ_h and ϵ_v such that $|\epsilon_h| < 1$ and $|\epsilon_v| < 1$. Then, if $\mathcal{K}$ and $\mathcal{K}_d$ have been determined independently,

$$\delta_{hh} = \frac{1}{\mathcal{K}\mathcal{K}_d} \frac{C_{hh}}{1-\epsilon_h^2}, \quad \delta_{hv} = -\frac{C_{hh}}{S_{hv}} \frac{1+\epsilon_h\epsilon_v}{1-\epsilon_h^2},$$

$$\delta_{vh} = -\frac{C_{hh}}{S_{vh}} \frac{1+\epsilon_h\epsilon_v}{1-\epsilon_h^2}, \quad \delta_{vv} = -\frac{C_{hh}}{C_{vv}} \frac{1-\epsilon_v^2}{1-\epsilon_h^2}. \tag{10}$$

The uncertainties in the Fourier coefficients C and S in Equation (7) can be obtained by examining the residuals of the Fourier analysis of the data and the lack of symmetries that the data exhibit. Details of this examination will not be presented here. In Equations (9) and (10) all the system parameters ϵ and δ are obtained in terms of the coefficients C and S in Equation (7). Consequently, the uncertainties in S and C can be propagated to obtain the uncertainties in ϵ and δ using basic rules of calculus [6]. Repeated measurements on different-sized dihedrals should provide the same system parameters within the stated uncertainties, thus providing us with a convenient consistency check on our results.

ERRORS AND UNCERTAINTIES IN RADAR CROSS SECTION MEASUREMENTS

Table 1 shows known sources of uncertainty [7] in RCS measurements for a set of radar system parameters as conceptualized at NIST; some of the most important sources

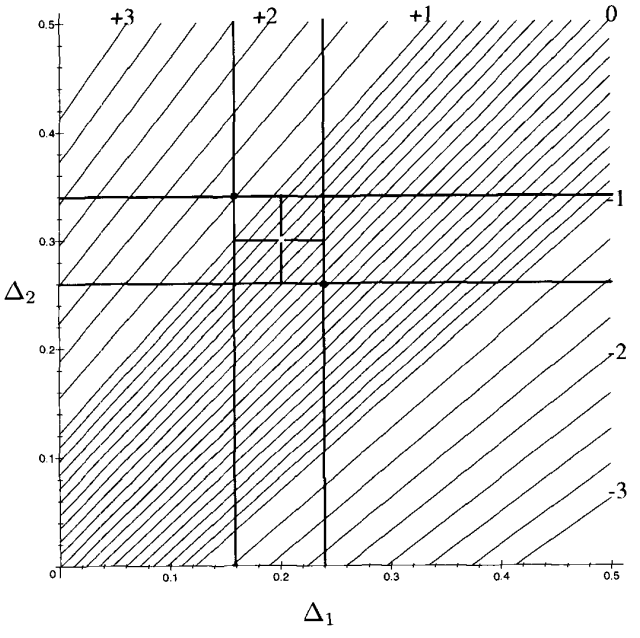

Figure 4. The decibel contours of *discrepancy* between measured and computed RCS as a function of fractional error fields. Contour levels in decibels are indicated on top and right edges of the plot. The upper and lower bounds of uncertainty as functions of the uncertainties $\delta\Delta_1$ and $\delta\Delta_2$ are also indicated.

To derive expressions for the uncertainty in the measured radar cross section discrepancy, as defined in Equation (14a), we assume that *best estimates* for $\Delta_i^0, i = 1, 2$ and their corresponding uncertainties $\delta\Delta_i$ have been determined successfully using fully documented theoretical, experimental, and/ or computational techniqes. Then Equation (14a) provides the best estimate for the discrepancy e_0,

$$e_0 \equiv \frac{\left|1+\Delta_2^0\right|^2}{\left|1+\Delta_1^0\right|^2}, \tag{16}$$

and the uncertainty in the best estimate of the discrepancy is determined by ordinary rules of propagation of uncertainties [6] for functions of two independent variables. However, it is very easy to write down the uncertainty bounds on the discrepancy in terms of the uncertainties $\delta\Delta_i$ in Δ_i,

$$\frac{\left|1+\Delta_2^0-\delta\Delta_2\right|^2}{\left|1+\Delta_1^0+\delta\Delta_1\right|^2} \leq \frac{\left|1+\Delta_2^0\right|^2}{\left|1+\Delta_1^0\right|^2} \leq \frac{\left|1+\Delta_2^0+\delta\Delta_2\right|^2}{\left|1+\Delta_1^0-\delta\Delta_1\right|^2}. \tag{17}$$

Figure 4 shows the uncertainty in the measured discrepancy. We assume here that all quantities are either positive and real, or that the complex phases are between 90° and $-90°$. Similar expressions can be easily derived if a different assumption is made.

We conclude with an important observation: *the uncertainty in the discrepancy is not, in general, the same as the uncertainty in the measured radar cross section.* The relationship between these uncertainties is given by [6]

$$\frac{\delta e}{e} = \frac{\delta\sigma}{\sigma} + \frac{\delta\sigma_c}{\sigma_c}, \tag{18}$$

where the last term is the fractional uncertainty in the *computed* radar cross section σ_c.

An example. We will now construct a simple example to demonstrate these ideas. *Assume* that the only error field in a RCS measurement system is the *background signal.* Then, in general,

$$\hat{E} = E^0 + \Delta E_b, \tag{19}$$

where $\hat{E}$, E^0, and ΔE_b are the *measured, ideal, and background signals,* as defined previously. After background subtraction, the *measured RCS* of the target cylinder is (see Equation (1))

$$\sigma_{i;j}(f) = \left|\frac{\hat{E}_i'(f) - \Delta E_b''}{\hat{E}_j'''(f) - \Delta E_b''''}\right|^2 \sigma_j^{(c)}(f), \tag{20}$$

where *primes* indicate the distinct times (here unspecified) the measurements were taken.

Let us assume that we have determined

(1) that the *best estimate* of the *residual background signal* after background subtraction is $\tilde{E}_b$ (indicating some systematic background effect), and

(2) that the uncertainty in background measurements is δE_b,

and, finally, let us assume

(3) that the ideal scattered field E^0 is known exactly, or that the uncertainty δE^0 is negligible.

Then, the *best estimate* of the discrepancy, according to Equation (16), is given by [6]

$$e_b^0 \equiv \frac{\left|1+\tilde{E}_b/E_2^0\right|^2}{\left|1+\tilde{E}_b/E_1^0\right|^2}. \tag{21}$$

Since the uncertainty in our measured signal after background subtraction is $2\delta E_b$ [6], the uncertainty bounds defined in Equation (17) are given by

$$\frac{\left|1+(\tilde{E}_b-2\delta E_b)/E_2^0\right|^2}{\left|1+(\tilde{E}_b+2\delta E_b)/E_1^0\right|^2} \le e_b^0 \le \frac{\left|1+(\tilde{E}_b+2\delta E_b)/E_2^0\right|^2}{\left|1+(\tilde{E}_b-2\delta E_b)/E_1^0\right|^2}. \quad (22)$$

SUMMARY

Equations (16) and (17) demonstrate how the uncertainty in the discrepancy between measured and exact theoretical radar cross sections can be determined. To implement these expressions, we need

(1) to determine the best estimate of the scattered electric field E^0 due to a plane wave illumination,

(2) to develop specific procedures to obtain best estimates of the various error signals present on an RCS measurement range, and

(3) to determine the uncertainties in the quantities obtained in steps (1) and (2).

One of the major *goals* of the national radar cross section standards and certification program, developed jointly by scientists from DoD, NIST, and industry, is to implement procedures that will determine the bounds specified in Equation (17). These procedures will be reported in the future.

Acknowledgements. I thank Robert Johnk and Dave Novotny, who are members of the RCS Measurement Working Group at NIST, and Byron Welsh, Mission Research, and Brian Kent, AFRL, WPAFB, who are active lead research scientists in RCS measurement technology, for useful comments and discussions. I also greatfully acknowledge partial support of this work by Mark Bushbeck, Boeing Phantom Works, Seattle, WA.

REFERENCES

[1] Smith, A. G., and Bryant, D. J., "Accuracy Requirements in Radar Cross Section Measurements from a System Viewpoint," *Correspondence, Proc. IEEE*, pp. 1159 – 1160, August, 1965.

[2] H. M. Chizever, R. J. Soerens and B. M. Kent, "On reducing primary calibration errors in radar cross section measurement," *Proc. Ant. Meas. Technique Assoc.*, pp. 383–388, Seattle, WA, Sept. 1996.

[3] Muth, L. A., Domich, P. D., Welsh, B. M., Buterbaugh, A. L. and Kent, B. M., "Polarimetric Calibration Standards for Monostatic Radar Systems," *Proceedings of NCSL Workshop and Symposium*, 1998.

[4] Brock, B. C., "Polarimetric calibration of a coherent measurement radar," *Tech. Rep. SAND91-2150 UC-706, Sandia National Laboratory*, December 1991.

[5] Whitt, M. W., Ulaby, F. T., Polatin, P. and Liepa, V. V., "A general polarimetric radar calibration technique," *IEEE Trans. Ant. Prop.*, vol. 39, pp. 62–67, 1991.

[6] Taylor, J. R., *An introduction to error analysis,* Sausalito, CA: University Science Books, 1982.

[7] Wittmann, R. C., Francis, M. H., Muth, L. A. and Lewis, R. L., "Proposed uncertainty analysis for RCS measurements," *Natl. Inst. Stand. Technol., Internal Report 5019*, 1994.

[8] Burnside, W. D., Gupta, I. J., Walton, E. K., and Young, J. D., "Some top down experiments for range characterization," *Proc. Ant. Meas. Technique Assoc.*, pp. 552 – 553, Boston, MA, Nov. 1997.

[9] Muth, L. A., Wittmann, R. C., and Kent, B. M., "Interlaboratory comparisons in radar cross section measurement assurance," *Proc. Ant. Meas. Technique Assoc.*, pp. 297 – 302, Boston, MA, Nov. 1997.

[10] Horn, R. A. and Johnson, C. R., *Topics in matrix analysis,* New York, NY: Cambridge University Press, 1991.